Performance Analysis and Code Optimization of Low Density Parity-Check Codes on Rayleigh Fading Channels

Jilei Hou, *Student Member, IEEE,* Paul H. Siegel, *Fellow, IEEE,* and Laurence B. Milstein, *Fellow, IEEE*

***Abstract*—A numerical method has recently been presented to determine the noise thresholds of low density parity-check (LDPC) codes that employ the message passing decoding algorithm on the additive white Gaussian noise (AWGN) channel. In this paper, we apply the technique to the uncorrelated flat Rayleigh fading channel. Using a nonlinear code optimization technique, we optimize irregular LDPC codes for such a channel. The thresholds of the optimized irregular LDPC codes are very close to the Shannon limit for this channel. For example, at rate one-half, the optimized irregular LDPC code has a threshold only 0.07 dB away from the capacity of the channel. Furthermore, we compare simulated performance of the optimized irregular LDPC codes and turbo codes on a land mobile channel, and the results indicate that at a block size of 3072, irregular LDPC codes can outperform turbo codes over a wide range of mobile speeds.**

***Index Terms*—Code optimization, density evolution, low-density parity-check codes, Rayleigh fading channels.**

I. Introduction

RECENT advances [1], [2] in error correcting codes have shown that, using the message passing decoding algorithm, irregular low density parity-check (LDPC) codes can achieve reliable transmission at signal-to-noise ratios (SNR) extremely close to the Shannon limit on the additive white Gaussian noise (AWGN) channel, outperforming turbo codes of the same block size and code rate. LDPC codes have certain advantages, such as simple descriptions of their code structure and fully parallelizable decoding implementations. With iterative message passing decoders, LDPC codes exhibit an interesting noise threshold effect [1]: if the noise level of the channel is smaller than a certain noise threshold, the bit error probability goes to zero as the block size goes to infinity; if the noise level is above the noise threshold, the probability of error is always bounded away from zero. Gallager [3] first presented this result for regular LDPC codes for the binary symmetric channel (BSC). Luby *et al.* [4] showed that the noise threshold effect also exists for irregular LDPC codes, and they designed some irregular LDPC codes whose performance is very close to the Shannon limit on the erasure channel. Richardson, *et al.* [1] generalized this idea to a variety of message passing decoding algorithms, including the full version of the belief propagation algorithm [5] which can be applied to a very broad class of binary-input symmetric channels, such as the AWGN channel. They developed a numerical technique, called *density evolution*, to analyze the performance of the belief propagation decoding algorithm, enabling the determination of noise thresholds to any desired degree of accuracy. In this paper, we apply this technique to the uncorrelated flat Rayleigh fading channel.

The code optimization of irregular LDPC codes is a nonlinear cost function minimization problem, a problem where differential evolution has been shown to be effective and robust [7]. This technique has been successfully applied to the design of good irregular LDPC codes for both the erasure channel [8] and the AWGN channel [2]. We show that this technique is also effective in the code optimization of irregular LDPC codes for the uncorrelated Rayleigh fading channel, and the threshold values of the optimized codes are extremely close to the capacity of this channel.

This paper is organized as follows. Section II briefly reviews the basic concepts of LDPC codes. In Section III, we review the decoding of LDPC codes and the technique of density evolution for threshold calculations on the AWGN channel. We then extend and apply this method to the uncorrelated flat Rayleigh fading channel. Section IV addresses two important properties related to the convergence of density evolution: symmetry and stability. We discuss the code optimization technique in Section V. In Section VI, we present the threshold calculations and code optimization results for the uncorrelated Rayleigh fading channel. We also compare simulation results for the optimized irregular LDPC codes and turbo codes on an uncorrelated, as well as correlated, Rayleigh fading channel. In Section VII, we present our conclusions.

II. Low Density Parity-Check (LDPC) Codes

An LDPC code is a linear block code specified by a very sparse parity-check matrix. As a linear block code, an LDPC code can be represented by a bipartite graph. Suppose the low density parity-check matrix H has N columns and M rows (the designed code rate $R = 1 - (M/N)$); the corresponding bipartite graph consists of N bit nodes, M check nodes, and a certain number of edges. Each bit node, called a "left node", represents a bit of the codeword. Each check node, called a "right node",

Manuscript received May 1, 2000; revised November 10, 2000. This work was supported by the National Science Foundation under Grant NCR-9725568. This paper was presented in part at the Thirty-Eighth Annual Allerton Conference on Communication, Control, and Computing, Monticello, IL, October 4–6, 2000.

The authors are with the Center for Wireless Communications, Dept. of Electrical and Computer Engineering, University of California, San Diego, La Jolla, CA 92093-0407 USA (e-mail: jhou@cwc.ucsd.edu, psiegel@cwc.ucsd.edu, milstein@ece.ucsd.edu).

Publisher Item Identifier S 0733-8716(01)03904-X.

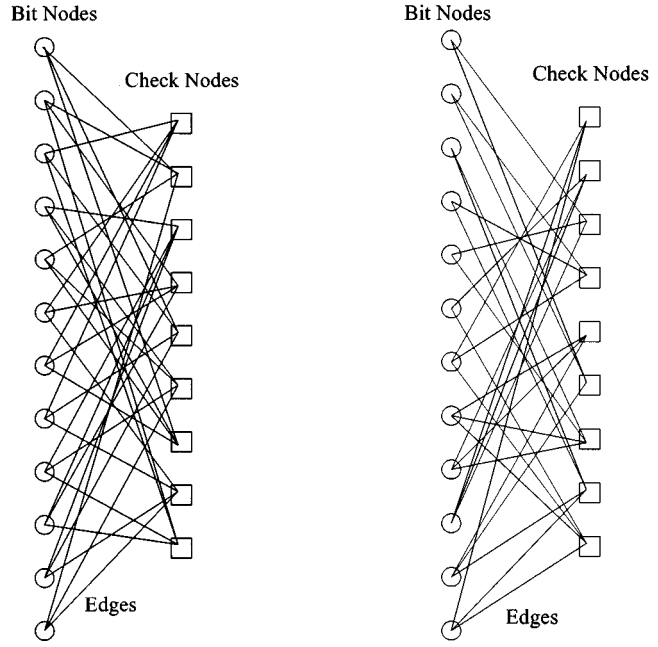

Fig. 1. Bipartite graph representations of LDPC codes.

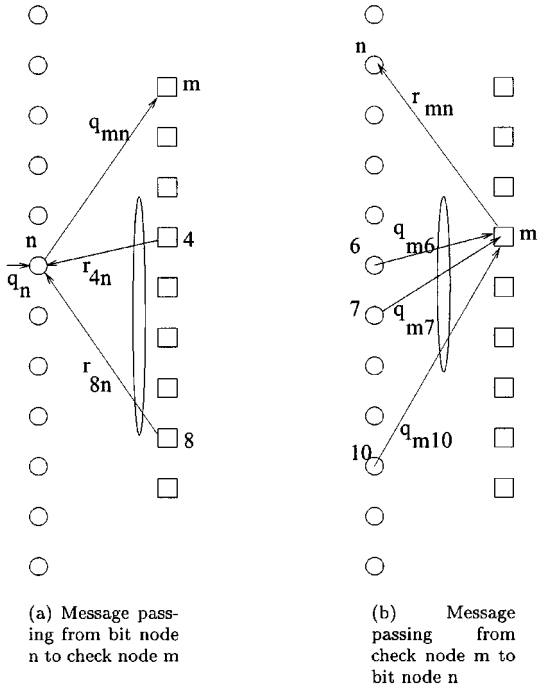

Fig. 2. Message passing decoder of LDPC codes.

represents a parity check of the code. An edge exists between a bit node and a check node if and only if there is a 1 in the corresponding entry in the parity-check matrix. We refer to the corresponding bit node and check node as the left and right neighbor nodes of the edge.

Regular LDPC codes are those for which all nodes of the same type have the same degree, where the degree of a node is the number of edges for which it is a neighbor node. A (j, k) regular LDPC code has a bipartite graph in which all bit nodes have degree j and all check nodes have degree k. Correspondingly, in the parity-check matrix H, all the column weights are j and all the row weights are k. Shown below is a parity-check matrix of a $(3, 4)$ regular LDPC code. Fig. 1(a) shows its associated bipartite graph.

$$H = \begin{bmatrix} 0 & 0 & 1 & 0 & 0 & 1 & 1 & 1 & 0 & 0 & 0 & 0 \\ 1 & 1 & 0 & 0 & 1 & 0 & 0 & 0 & 0 & 0 & 0 & 1 \\ 0 & 0 & 0 & 1 & 0 & 0 & 0 & 0 & 1 & 1 & 1 & 0 \\ 0 & 1 & 0 & 0 & 0 & 1 & 1 & 0 & 0 & 1 & 0 & 0 \\ 1 & 0 & 1 & 0 & 0 & 0 & 0 & 1 & 0 & 0 & 1 & 0 \\ 0 & 0 & 0 & 1 & 1 & 0 & 0 & 0 & 1 & 0 & 0 & 1 \\ 1 & 0 & 0 & 1 & 1 & 0 & 1 & 0 & 0 & 0 & 0 & 0 \\ 0 & 0 & 0 & 0 & 0 & 1 & 0 & 1 & 0 & 0 & 1 & 1 \\ 0 & 1 & 1 & 0 & 0 & 0 & 0 & 0 & 1 & 1 & 0 & 0 \end{bmatrix}$$

For irregular LDPC codes, the bit nodes (correspondingly the check nodes) can have different degrees. We say an edge has left (resp., right) degree i if its left (resp., right) neighbor node has degree i. An irregular LDPC code ensemble is specified by a degree distribution pair (λ, ρ) or its corresponding generating functions $\lambda(x) = \sum_{i=2}^{d_{l\max}} \lambda_i x^{i-1}$ and $\rho(x) = \sum_{i=2}^{d_{r\max}} \rho_i x^{i-1}$, where λ_i (resp., ρ_i) is the fraction of edges with left (resp., right) degree i and $d_{l\max}$ (resp., $d_{r\max}$) is the maximal left (resp., right) degree of any edge. The bipartite graph for an irregular LDPC code is shown in Fig. 1(b), where $\lambda_2 = 0.4, \lambda_3 = 0.6, \rho_3 = 0.6$, and $\rho_4 = 0.4$. The intuition behind the use of irregular LDPC codes is quite simple: in the decoding process of irregular LDPC codes, there exists a phenomenon called the "wave effect" [4], whereby the bit nodes with high degrees tend to approach their correct values very quickly, and in turn, they provide more reliable information to the check nodes and subsequently to the bit nodes with lower degrees.

III. Decoding Analysis

The decoding algorithm for LDPC codes is based on the idea of belief propagation [5]. As described in [2] and [9], for each edge of the underlying bipartite graph, the decoding algorithm iteratively updates two types of log *a posteriori* probability ratio (LAPPR) messages, q and r. The quantity q is the message sent from the bit node to the check node along a connecting edge e, which is expressed as $q = \log(p(x = 0 \,|\, t)/p(x = 1 \,|\, t))$, where x denotes the value of the bit node, and t denotes all the messages coming from the channel and the edges connected to the bit node, other than edge e. The quantity r is the message sent from the check node to the bit node along an edge e, which is defined as $r = \log(p(x = 0 \,|\, v)/p(x = 1 \,|\, v))$, where v denotes the messages coming from the edges connected to the check node, other than edge e. It is important to note that during the message updating, the incoming message along edge e is excluded in determining the outgoing message along edge e. That is, similar to turbo decoding [10], only *extrinsic* information is circulated, which turns out to be an important property of good message passing decoders and which also makes the analysis of the decoding algorithm feasible [1]. Fig. 2 illustrate the basic operations in the decoding algorithm.

After l such iterations, the algorithm would produce the exact LAPPRs of all the bits if the bipartite graph defined by the

parity-check matrix contains no loops of length up to $2l$ [9]. If we assume that the graph is loop-free, we can analyze the decoding algorithm directly because the incoming messages to every node are independent. Also, by the general concentration theorem of [1], for almost all the graphs in a code ensemble (λ, ρ) and almost all inputs, the decoder performance will converge to that of a corresponding loop-free graph as the codeword length approaches infinity.

Based on the assumption above, the following decoding analysis tries to track the *average* fraction of incorrect messages that is passed in each iteration of the decoding algorithm. Here, the fraction of incorrect messages is averaged over all the bits of a codeword.

First, we consider a regular (j, k) LDPC code. Using the fact that LDPC codes are linear block codes and both the channel and the decoding algorithm considered are symmetric [1], we assume that the all-zero codeword is sent. Assuming BPSK modulation $(0 \rightarrow 1, 1 \rightarrow -1)$, it is easy to see that the fraction of incorrect messages that is passed is equal to the fraction of messages with negative signs. Considering the message passed from the bit node to the check node, we have [2]

$$q = q_0 + \sum_{i=1}^{j-1} r_i \tag{1}$$

where q_0 is the initial message conditioned on the channel output, and $r_i, i = 1, \ldots, j-1$, are the incoming LAPPR messages from all the incident edges, other than edge e. Since q_0 and r_i are all random variables, the density function of q is the convolution of the density functions of all the elements in (1). This convolution can be efficiently computed in the Fourier domain. Let P_0 denote the density of q_0, P_l denote the density of q after l iterations, and R_l denote the density of r after l iterations. Letting F denote the Fourier transform operation

$$P_l = F^{-1}(F(P_0)(F(R_{l-1}))^{j-1}) \tag{2}$$

where $R_0(r)$ can be set to Δ_0, and Δ_0 is defined as 1 if $r = 0$ and 0 if $r \neq 0$. We can write $P_l = P_l^1 + P_l^0$, where P_l^1 is supported on $(-\infty, 0]$ and P_l^0 is supported on $[0, \infty)$. Therefore, the fraction of incorrect messages after l iterations can be defined as[1]

$$Pe(l) = \int_{-\infty}^{0} P_l(z)\, dz. \tag{3}$$

On the other hand, considering the message r passed from the check node to the bit node r, we have [2]

$$\tanh \frac{r}{2} = \prod_{i=1}^{k-1} \tanh \frac{q_i}{2} \tag{4}$$

where $q_i, i = 1, \ldots, k-1$ are the incoming LAPPRs from the neighbor edges, other than edge e. To use the same method as described for the bit node to calculate the density function R_l, we need to apply logarithm operations on both sides of (4) to change the product into the pair of summations

$$\mathrm{sgn}_r = \sum_{i=1}^{k-1} \mathrm{sgn}_{q_i} (\mathrm{mod}\, 2)$$

and

$$\log \left| \tanh \frac{r}{2} \right| = \sum_{i=1}^{k-1} \log \left| \tanh \frac{q_i}{2} \right| \tag{5}$$

where the sign function $\mathrm{sgn}_x = 0$ if $x \geq 0$, and $\mathrm{sgn}_x = 1$ otherwise. Note that the summation for (5) is the mod-2 summation of the sign parts and the real summation of the magnitude parts. Therefore, the density of r can be computed in the Fourier domain in a manner similar to the computation of the density of q in (2).

This two-phase computation algorithm, called density evolution, makes it possible to track the fraction of incorrect messages, $Pe(l)$. At a certain noise level, we can run this algorithm iteratively until the error probability $Pe(l)$ either goes to zero or stops at a finite probability of error. The noise threshold, σ^*, denotes the supremum of all values of the noise level σ such that $\lim_{l \rightarrow \infty} Pe(l) = 0$, where σ is the standard deviation of the noise.

The density evolution algorithm can be extended to the irregular LDPC codes with only minor modifications, taking into consideration the irregular degree distribution pair. For example, at a bit node, we have

$$P_l = F^{-1}(F(P_0) \cdot \lambda(F(R_{l-1}))) \tag{6}$$

where $\lambda(x) = \sum_{i=2}^{d_{l\max}} \lambda_i x^{i-1}$ is as defined above. In the following, we briefly review the application of the algorithm above to the AWGN channel, and then show how to apply it to the uncorrelated Rayleigh fading channel.

A. AWGN

If the code symbol x is mapped into the signal point $w = (1-2x)$, the sampled matched filter output y has the conditional probability density function (pdf)

$$p(y \,|\, w) = \frac{1}{\sqrt{2\pi\sigma^2}} \exp\left(-\frac{(y-w)^2}{2\sigma^2} \right) \tag{7}$$

where $\sigma^2 = (1/2R \cdot (E_b/N_0))$ is the variance of the noise, and R is the code rate. Assuming $Pr(x=0) = Pr(x=1) = 1/2$, the message observed from the channel can be expressed as

$$q_0 = \log \frac{P(x=0 \,|\, y)}{P(x=1 \,|\, y)} = \frac{2}{\sigma^2} y. \tag{8}$$

In the decoding analysis, since we assume the all-zero codeword is sent, i.e., $w = 1$, a change of variable in (7) yields the density function of q_0:

$$P_0(q_0) = \frac{\sigma}{2\sqrt{2\pi}} \exp\left(-\frac{\left(q_0 - \frac{2}{\sigma^2}\right)^2}{2(4/\sigma^2)} \right) \tag{9}$$

[1]In general, if density function P_l has a point mass at zero, half of the mass should be included into $Pe(l)$.

which is a Gaussian density with mean $2/\sigma^2$ and variance $4/\sigma^2$, and this density function can be used in the density evolution analysis.

B. Uncorrelated Rayleigh Fading

For the uncorrelated Rayleigh fading channel, the conditional pdf of the matched filter output y is

$$p(y\,|\,w,a) = \frac{1}{\sqrt{2\pi\sigma^2}} \exp\left(-\frac{(y-w\cdot a)^2}{2\sigma^2}\right) \tag{10}$$

where a is the normalized Rayleigh fading factor with $E[a^2] = 1$ and density function $p(a) = 2a\exp(-a^2)$.

1) Ideal Side Information (SI): When we have ideal SI, the initial message passed from the bit node to the check node is

$$q_0 = \log\frac{P(x=0\,|\,y,a)}{P(x=1\,|\,y,a)} = \frac{2}{\sigma^2}y\cdot a. \tag{11}$$

In the decoding analysis, assuming $w = 1, q_0$ has the conditional density function

$$P_0(q_0\,|\,a) = \frac{\sigma}{2a\sqrt{2\pi}} \exp\left(-\frac{\left(q_0 - \frac{2a^2}{\sigma^2}\right)^2}{8a^2/\sigma^2}\right). \tag{12}$$

To get the unconditional density function of q_0, we average (12) over the density function of a, so that

$$\begin{aligned} P_0(q_0) &= \int_0^\infty \frac{\sigma}{\sqrt{2\pi}} \exp\left(-\frac{\left(q_0 - \frac{2a^2}{\sigma^2}\right)^2}{8a^2/\sigma^2}\right)\exp(-a^2)\,da \\ &= \frac{\sigma}{\sqrt{2\pi}}\exp\left(\frac{-q_0(\sqrt{2\sigma^2+1}-1)}{2}\right) \\ &\quad\times\int_0^\infty \exp\left(-\frac{\left(\frac{\sigma^2}{2a}q_0 - a\sqrt{2\sigma^2+1}\right)^2}{2\sigma^2}\right)da. \end{aligned} \tag{13}$$

2) No Side Information (No SI): When no SI is available, following [11], we assume that $P(y\,|\,w)$ is Gaussian distributed in the region of the most probable y, and we approximate q_0 as

$$q_0 \approx \frac{2}{\sigma^2}y\cdot E[a], \tag{14}$$

where $E[a] = 0.8862$. The corresponding conditional density function is

$$P_0(q_0\,|\,a) = \frac{\sigma}{2E[a]\sqrt{2\pi}} \exp\left(-\frac{\left(q_0 - \frac{2aE[a]}{\sigma^2}\right)^2}{8(E[a])^2/\sigma^2}\right). \tag{15}$$

Averaging over the density function of a, we get

$$\begin{aligned} P_0(q_0) &= \frac{\sigma\Delta^2}{2E[a]}\exp\left(-\frac{\Delta^2\sigma^2q_0^2}{4(E[a])^2}\right) \\ &\quad\times\left[\sqrt{\frac{2}{\pi}}\exp\left(-\frac{\Delta^2q_0^2}{8(E[a])^2}\right) + \frac{\Delta q_0}{E[a]}Q\left(\frac{-\Delta q_0}{2E[a]}\right)\right], \end{aligned} \tag{16}$$

where $\Delta = \sqrt{\sigma^2/(2\sigma^2+1)}$ and $Q(x) = (1/2)\operatorname{erfc}(x/\sqrt{2})$.

IV. Symmetry and Stability

Symmetry is an important property associated with the message distribution in the density evolution of belief propagation. As defined in [2], a density function f on $[-\infty,\infty]$ is symmetric if it satisfies $f(x) = f(-x)e^x$ for all $x\in[0,\infty]$, and it is shown that the initial message distributions for all the binary-input symmetric channels discussed in [2] satisfy this condition. For the initial message density function of the AWGN channel, (9), it is easy to verify that

$$\begin{aligned} P_0(q_0) &= \frac{\sigma}{2\sqrt{2\pi}}\exp\left(-\frac{\left(q_0-\frac{2}{\sigma^2}\right)^2}{2(4/\sigma^2)}\right) \\ &= \frac{\sigma}{2\sqrt{2\pi}}\exp\left(-\frac{\left(-q_0-\frac{2}{\sigma^2}\right)^2}{2(4/\sigma^2)}\right)\exp(q_0) \\ &= P_0(-q_0)e^{q_0}. \end{aligned} \tag{17}$$

It was shown in [2] that the symmetry property is invariant under density evolution, i.e., if P_0 is symmetric, then the density functions of P_l and R_l calculated in density evolution are also symmetric. It was next proved in [2] that if the density function of P_l is symmetric, the average fraction of incorrect messages as defined in (3) is a nonincreasing function of l and will always converge to a certain value, which might be zero.

In [2], the symmetry property is then used to prove another important property of density evolution, which is summarized as follows: There exists an $\varepsilon > 0$ such that if density evolution is initialized with a symmetric message density P_0 satisfying $\int_{-\infty}^0 P_0(x)\,dx < \varepsilon$, the fraction of incorrect messages will converge to zero under density evolution if

$$\lambda'(0)\rho'(1) < e^s \tag{18}$$

where the parameter s is defined as

$$s = -\log\left(2\int_0^\infty P_0(x)e^{-x/2}\,dx\right). \tag{19}$$

Conversely, if $\lambda'(0)\rho'(1) > e^s$, then the fraction of incorrect messages is strictly bounded away from 0.

In [2], (18) is referred to as the stability condition for the channel with initial message density P_0. For example, for the AWGN channel, the stability condition is given by [2]

$$\lambda'(0)\rho'(1) < e^{\frac{1}{2\sigma^2}}. \tag{20}$$

We now show that the initial message density function of the uncorrelated Rayleigh fading channel with SI also satisfies the symmetry property, and then we derive the stability condition for this channel. For the density function of the uncorrelated Rayleigh fading channel with SI, as defined in (13), it is easily verified that

$$\begin{aligned} P_0(q_0) &= \int_0^\infty \frac{\sigma}{\sqrt{2\pi}} \exp\left(-\frac{\left(q_0 - \frac{2a^2}{\sigma^2}\right)^2}{8a^2/\sigma^2}\right) \exp(-a^2)\, da \\ &= \exp(q_0) \int_0^\infty \frac{\sigma}{\sqrt{2\pi}} \\ &\quad \times \exp\left(-\frac{\left(-q_0 - \frac{2a^2}{\sigma^2}\right)^2}{8a^2/\sigma^2}\right) \exp(-a^2)\, da \\ &= P_0(-q_0)\exp(q_0). \end{aligned} \tag{21}$$

That is, the initial message density function of the uncorrelated Rayleigh fading channel with SI satisfies the symmetry condition. From (19) and (13), we have

$$\begin{aligned} e^{-s} &= 2\int_0^\infty P_0(q_0) e^{-q_0/2}\, dq_0 \\ &= 2\int_0^\infty da \frac{\sigma}{\sqrt{2\pi}} e^{-a^2} \\ &\quad \times \int_0^\infty \exp\left(-\frac{\left(q_0 - \frac{2a^2}{\sigma^2}\right)^2}{8a^2/\sigma^2}\right) e^{-q_0/2}\, dq_0 \\ &= \int_0^\infty 2a \exp\left(-\left(1 + \frac{1}{2\sigma^2}\right)a^2\right) da \\ &= 1 \Big/ \left(1 + \frac{1}{2\sigma^2}\right), \end{aligned} \tag{22}$$

i.e., the stability condition for the uncorrelated Rayleigh fading channel with SI is

$$\lambda'(0)\rho'(1) < 1 + \frac{1}{2\sigma^2}. \tag{23}$$

In the next section, we will numerically optimize the degree distribution pair for this channel, and we will verify empirically that they fulfill condition (23). As to the Rayleigh fading channel without SI, the initial density function (16) does not have the symmetry property. This is because the expression (14) for the message, q_0, is only an approximation. Nevertheless, as shown in the numerical results, the density evolution technique for determining the thresholds still works quite well for this channel.

V. Code Optimization: Differential Evolution

Since we can determine the threshold value for each LDPC code ensemble defined by its degree distribution pair (λ, ρ), we try to find the degree distribution pair which yields the largest possible noise threshold for a given channel. This problem is a nonlinear cost function minimization problem with continuous space parameters, a problem where differential evolution has been shown to be effective and robust [7]. This technique has been successfully applied to the design of good irregular LDPC codes for both the erasure channel [8] and the AWGN channel [2]. For the AWGN channel, Richardson *et al.* [2] found the best degree distribution pair for rate-$1/2$ codes, which has a threshold within 0.06 dB of capacity! We now show that this method is also very effective in the design of good irregular LDPC codes for a Rayleigh fading channel with SI.

Before describing the differential evolution technique, we need to remove the dependencies among the components of the degree distribution pair. It is easy to verify that the degree distribution pair (λ, ρ) satisfies the following constraint

$$\sum_i \frac{\rho_i}{i} = K \sum_i \frac{\lambda_i}{i} \tag{24}$$

where $K = 1 - R$ and R is the code rate. Also, we have

$$\lambda_2 = 1 - \sum_{i=3}^{d_{l\max}} \lambda_i, \quad \rho_2 = 1 - \sum_{i=3}^{d_{r\max}} \rho_i. \tag{25}$$

Using (24) and (25) to solve for $\lambda_{d_{l\max}}$ gives (26), shown at the bottom of the page.

Next, let L denote the number of free elements of the degree distribution pair (λ, ρ). The dependences (25) and (26), combined with the fact that $\lambda_1 = \rho_1 = 0$, show that $L = d_{l\max} + d_{r\max} - 5$. We form an L-dimensional parameter vector $\mathbf{p} = (\lambda_3, \ldots, \lambda_{d_{l\max}-1}, \rho_3, \ldots, \rho_{d_{r\max}})$, and our goal is to optimally choose the elements of this vector so that the corresponding degree distribution pair yields the largest noise threshold.

Differential evolution is a parallel direct search technique. Starting from an initial set of vectors, the algorithm iteratively updates each vector in the set simultaneously until a superior vector is found which has the best cost function value. By updating all the vectors of the set in parallel, the algorithm can help the vectors escape local minima and prevent misconvergence. The differential evolution algorithm that we used in the code optimization is based on [8] with minor modifications. In the following, we briefly review it.

1) Initialization — We start with a certain noise level σ, which is the standard deviation of the noise. For the first generation $G = 0$, we randomly choose NP L-dimensional vectors $\mathbf{p}_{i,G}, i = 0, 1, \ldots, NP-1$, where $NP = 10L$ is a constant that remains fixed during the optimization process [7]. For each vector $\mathbf{p}_{i,G}$, we run the den-

$$\lambda_{d_{l\max}} = \frac{\frac{1-K}{2} + \sum_{i=3}^{d_{r\max}} \rho_i \left(\frac{1}{i} - \frac{1}{2}\right) - K \sum_{i=3}^{d_{l\max}-1} \lambda_i \left(\frac{1}{i} - \frac{1}{2}\right)}{K\left(\frac{1}{d_{l\max}} - \frac{1}{2}\right)}. \tag{26}$$

sity evolution as discussed in Section III for a certain number of iterations (e.g., 1000) and record its residual error $Pe_{i,G}$, i.e., the fraction of incorrect messages as defined by (3). We label the vector with the smallest $Pe_{i,G}$ as the best vector, $\mathbf{p}_{\text{best},G}$.

2) Mutation — For the next generation, $G+1$, new vectors are generated according to the following mutation scheme. For each $i = 0, 1, \ldots, NP-1$, randomly choose distinct integers $r1, r2, r3$ and $r4$ from $[0, NP-1]$, each different from the index i, and define

$$\mathbf{v}_{i,G+1} = \mathbf{p}_{\text{best},G} + F(\mathbf{p}_{r1,G} - \mathbf{p}_{r2,G} + \mathbf{p}_{r3,G} - \mathbf{p}_{r4,G}) \quad (27)$$

where F is a real constant which controls the amplification of the differential variation. We choose $F = 0.5$ in our optimization [8]. The use of two vector differences increases the variation, thereby helping to prevent the algorithm from getting into a local minimum. For each new vector, we run the density evolution for the same number of iterations and record its residual error, $Pv_{i,G+1}$.

3) Selection — For each $i = 0, 1, \ldots, NP-1$, compare $Pe_{i,G}$ and $Pv_{i,G+1}$. If $Pe_{i,G}$ is larger than $Pv_{i,G+1}, \mathbf{p}_{i,G+1}$ is set to $\mathbf{v}_{i,G+1}$. Otherwise, $\mathbf{p}_{i,G+1}$ is set to $\mathbf{p}_{i,G}$. We denote the vector with the smallest residual error by $\mathbf{p}_{\text{best},G+1}$.

4) Stopping criterion — If the residual error $Pe_{\text{best},G+1}$ of the vector $\mathbf{p}_{\text{best},G+1}$ is not zero (practically, if it is not less than a very small value, e.g., 10^{-8}), return to step 2. Otherwise, increase the noise level σ slightly, and return to step 1. If the noise level is increased to a value for which the residual error of the best vector does not converge to zero after a very long running time, the process is stopped. We label the vector whose residual error goes to zero at the highest possible noise level as the best vector, and the corresponding noise level as the noise threshold σ^*.

VI. Results

A. Threshold Calculation and Code Optimization

Using the density evolution technique discussed in Section III, we can calculate the threshold values of LDPC codes for both the AWGN channel and the uncorrelated Rayleigh fading channel with or without SI. For convenience, in the following results, we will express the threshold by both σ and its corresponding (E_b/N_0) (dB). Since $\sigma^2 = (1/2R \cdot (E_b/N_0))$, the threshold can also be defined as the smallest E_b/N_0 such that $\lim_{l\to\infty} Pe(l) = 0$. Fig. 3 compares the thresholds and the simulation results of rate-$1/2$ regular $(3,6)$ LDPC codes on both the AWGN channel and the uncorrelated Rayleigh fading channel, where both ideal SI and no SI are considered. As shown, the thresholds for regular $(3,6)$ LDPC codes on the AWGN channel, the fading channel with SI, and the fading channel with no SI, are 1.10 dB, 3.06 dB, and 4.06 dB, respectively. The $(3,6)$ LDPC codes used in the simulations are of block size[2] 10^5 and 10^6. The numerical threshold results are very consistent with the simulation results, and we

[2]In the simulation results, the block size used is codeword block size.

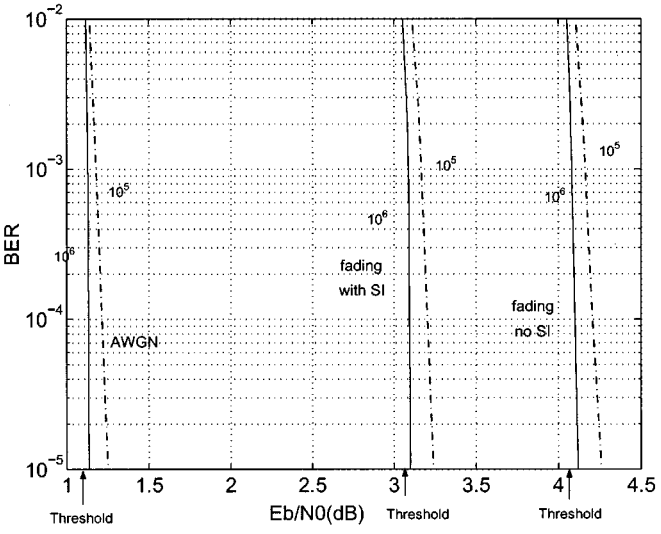

Fig. 3. Comparison of thresholds and simulation results for rate-$1/2$, $(3,6)$ regular LDPC codes on the AWGN channel, and the uncorrelated Rayleigh fading channels with or without SI. The codes used in simulations are of block size 10^5 and 10^6.

conjecture that as the block size goes to infinity, the simulation results will converge to the thresholds. If the conjecture is true, the threshold can be considered as the capacity of the corresponding code parameters, i.e., the best performance that such an LDPC code can achieve with the message passing decoder. The results show that the regular $(3,6)$ LDPC code suffers a loss of nearly 2 dB and 3 dB, respectively, in the fading channels with SI and without SI, relative to the AWGN channel.

Combining the density evolution and differential evolution techniques as described above, we searched for good degree distribution pairs with constraints on the maximal left degree $d_{l\max}$ for the uncorrelated Rayleigh fading channel with SI. Similar to what has been observed for the erasure channel [8] and the AWGN channel [2], we found that for the fading channel with SI, good degree distribution pairs exist with only a few nonzero terms. Therefore, in the results shown, we use only three consecutive nonzero right degrees and limit the nonzero degrees on the left to the degrees 2, 3, $d_{l\max}$, and several carefully chosen degrees in-between, which greatly reduces the search space and consequently saves on search time.

The resulting degree distribution pairs of rate-$1/2$ codes for the Rayleigh fading channel with SI are shown in Table I for $d_{l\max} = 10, 20, 30$, and 50. Each column corresponds to one particular degree distribution pair. For each degree distribution pair, the coefficients of λ and ρ are given, as well as the noise threshold σ^*, and the corresponding $(E_b/N_0)^*$ in dB. Also listed is λ_2^*, the maximal value of λ_2 satisfying the stability condition (23). As can be seen, $\lambda_2 < \lambda_2^*$ for every degree distribution pair in the table, which confirms that these degree distribution pairs satisfy the stability condition. Also, the higher the maximal left degree, the better the performance of the code.

Similar to the results that Richardson *et al.* [2] obtained for the AWGN channel, the thresholds of the degree distribution pairs optimized for the fading channel with SI are very close to the capacity of this channel (the capacity can be calculated following

TABLE I
GOOD DEGREE DISTRIBUTION PAIRS OF RATE-$1/2$ FOR THE UNCORRELATED RAYLEIGH FADING CHANNELS WITH SI AND WITH CONSTRAINTS ON THE MAXIMAL LEFT DEGREES $d_{l\max} = 10, 20, 30$ AND 50. FOR EACH DISTRIBUTION PAIR THE NOISE THRESHOLD VALUE σ^* AND THE CORRESPONDING $(E_b/N_0)^*$ (dB) ARE GIVEN. THE MAXIMAL VALUE OF λ_2 SATISFYING CONDITION (23), λ_2^*, IS GIVEN FOR $\sigma = \sigma^*$ AND THE GIVEN $\rho'(1)$. NOTE THAT THE CAPACITY FOR THIS CHANNEL AT CODE RATE $1/2$ IS 1.830 dB

d_{lmax}	10	20	30	50
λ_2^*	0.300932	0.253856	0.229439	0.204885
λ_2	0.292439	0.246544	0.220033	0.194255
λ_3	0.253636	0.230609	0.222611	0.206322
λ_4	0.060454	0.002045	0.000100	0.000111
λ_6		0.046487	0.000919	
λ_7		0.150161	0.069962	0.092232
λ_8		0.035344	0.201925	0.111427
λ_9	0.031610			0.014172
λ_{10}	0.361861			
λ_{15}			0.000531	0.113788
λ_{19}		0.004812		
λ_{20}		0.283998		
λ_{29}			0.001791	
λ_{30}			0.282128	0.001514
λ_{49}				0.003503
λ_{50}				0.262676
ρ_6	0.007254			
ρ_7	0.979220	0.000952		
ρ_8	0.013526	0.951871	0.254080	
ρ_9		0.047177	0.739388	0.346906
ρ_{10}			0.006532	0.645429
ρ_{11}				0.007665
σ^*	0.7869	0.7962	0.8013	0.8035
$\left(\frac{E_b}{N_0}\right)^*$ dB	2.082	1.980	1.924	1.900

the method introduced in [12]). At rate $1/2$, the capacity of the fading channel with SI is 1.830 dB. The degree distribution pair with $d_{l\max} = 50$ has the threshold of 1.900 dB, which is only 0.07 dB away from the capacity! Compared to the regular $(3, 6)$ LDPC code whose threshold on this channel is 3.06 dB, optimized irregular LDPC codes have much better thresholds.

It is interesting to see how the degree distribution pairs optimized for the fading channel with SI perform on the AWGN channel, and vice-versa. We compare the rate-$1/2$ degree distribution pairs optimized for the AWGN channel (refer to [2] for the detailed degree distribution pairs) and the degree distribution pairs optimized for the fading channel with SI in Figs. 4 and 5. In Fig. 4, for each degree distribution pair, we show the gap between its threshold value for the AWGN channel and the AWGN channel capacity for rate $1/2$. In Fig. 5, for each degree distribution pair, we show the gap between its threshold value for the fading channel with SI and the capacity for that channel for rate $1/2$. It can be seen that the degree distribution pairs optimized for the fading channel with SI are also very good distribution pairs on the AWGN channel, e.g., considering the degree distribution pair with $d_{l\max} = 50$ optimized for the fading channel with SI, its threshold value for the AWGN channel is only 0.18 dB away from the channel capacity. Similar results can be observed from Fig. 5 for the converse situation. As suggested in [4], in the construction of block codes, it is better to have high degree for the bit nodes, since the more information a bit node

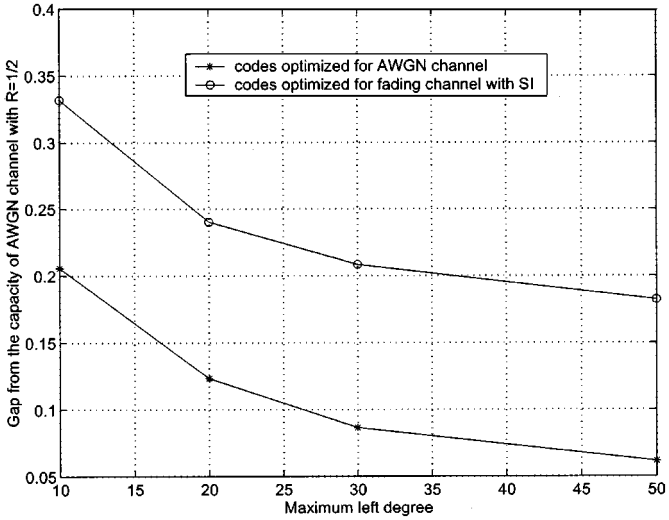

Fig. 4. Comparison of the threshold values on the AWGN channel of the rate-$1/2$ degree distribution pairs optimized for the AWGN channel and the fading channel with SI. For each distribution pair, the gap between its threshold value for the AWGN channel and the capacity of this channel is shown. Note that the capacity for the AWGN channel at rate $1/2$ is 0.1870 dB.

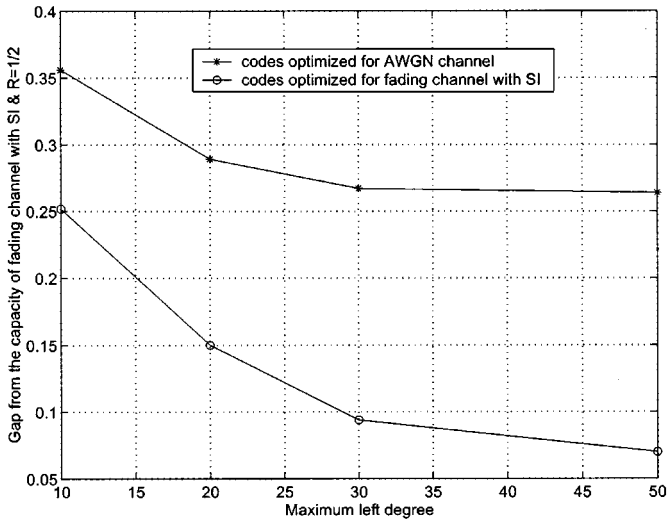

Fig. 5. Comparison of the threshold values on the fading channel with SI of the rate-$1/2$ degree distribution pairs optimized for the AWGN channel and the fading channel with SI. For each distribution pair, the gap between its threshold value for the fading channel with SI and the capacity of this channel is shown. Note that the capacity for the fading channel with SI at rate $1/2$ is 1.830 dB.

gets from its check nodes, the more reliably it can provide its own correct value. On the other hand, it is better for a check node to have low degree, in order to provide more accurate information to its bit nodes. These two competing requirements will have different balances for different channels. The degree distribution pair with $d_{l\max} = 50$ optimized for the AWGN channel [2] has average right degree 10.24. However, the degree distribution pair with $d_{l\max} = 50$ optimized for the fading channel with SI has average right degree 9.66. The results suggest that, compared to the AWGN channel, the fading channel with SI favors lower average right degree. The same relations can be observed for the degree distribution pairs with $d_{l\max} = 10, 20$, and 30.

Tables II and III give the rate-$1/3$ degree distribution pairs we optimized for the AWGN channel and the uncorrelated Rayleigh

TABLE II
GOOD DEGREE DISTRIBUTION PAIRS OF RATE-$1/3$ FOR THE AWGN CHANNELS AND WITH CONSTRAINTS ON THE MAXIMAL LEFT DEGREES $d_{l\max} = 10, 16, 30$ AND 50. FOR EACH DISTRIBUTION PAIR THE NOISE THRESHOLD VALUE σ^* AND THE CORRESPONDING $(E_b/N_0)^*$ (dB) ARE GIVEN. THE MAXIMAL VALUE OF λ_2 SATISFYING CONDITION (20), λ_2^*, IS GIVEN FOR $\sigma = \sigma^*$ AND THE GIVEN $\rho'(1)$. NOTE THAT THE CAPACITY FOR THIS CHANNEL AT CODE RATE $1/3$ IS -0.4954 dB.

d_{lmax}	10	16	30	50
λ_2^*	0.342056	0.298223	0.264470	0.237297
λ_2	0.329076	0.287567	0.256988	0.225792
λ_3	0.261590	0.230039	0.217847	0.207865
λ_4	0.048686	0.002147		0.012662
λ_5		0.068969		
λ_6		0.095590		
λ_7			0.163553	0.107496
λ_8		0.019108	0.061250	0.064003
λ_9			0.044084	0.032510
λ_{10}	0.360648		0.001780	0.012288
λ_{15}				0.100307
λ_{16}		0.296580		
λ_{29}			0.002474	
λ_{30}			0.252024	0.030314
λ_{50}				0.206763
ρ_4	0.000294	0.003426		
ρ_5	0.998683	0.424437		
ρ_6	0.001023	0.572137	0.882069	0.349540
ρ_7			0.114372	0.598609
ρ_8			0.003559	0.051851
σ^*	1.2625	1.2714	1.2837	1.2858
$\left(\frac{E_b}{N_0}\right)^* dB$	-0.2637	-0.3247	-0.4084	-0.4225

TABLE III
GOOD DEGREE DISTRIBUTION PAIRS OF RATE-$1/3$ FOR THE UNCORRELATED RAYLEIGH FADING CHANNEL WITH SI AND WITH CONSTRAINTS ON THE MAXIMAL LEFT DEGREES $d_{l\max} = 10, 16, 30$ AND 50. FOR EACH DISTRIBUTION PAIR THE NOISE THRESHOLD VALUE σ^* AND THE CORRESPONDING $(E_b/N_0)^*$ (dB) ARE GIVEN. THE MAXIMAL VALUE of λ_2 SATISFYING CONDITION (23), λ_2^*, IS GIVEN FOR $\sigma = \sigma^*$ AND THE GIVEN $\rho'(1)$. NOTE THAT THE CAPACITY FOR THIS CHANNEL AT CODE RATE $1/3$ IS 0.4885 dB.

d_{lmax}	10	16	30	50
λ_2^*	0.351321	0.312740	0.279123	0.248068
λ_2	0.328411	0.298433	0.267474	0.237738
λ_3	0.300171	0.245016	0.228605	0.200028
λ_4	0.001721			0.026700
λ_5		0.007173		
λ_6	0.001274	0.167659		
λ_7			0.140199	0.094505
λ_8			0.054426	0.050632
λ_9	0.000662		0.063206	0.028717
λ_{10}	0.367760		0.006163	0.060597
λ_{15}				0.057204
λ_{16}		0.281719		
λ_{29}			0.029347	
λ_{30}			0.210580	0.053621
λ_{49}				0.174248
λ_{50}				0.016010
ρ_4	0.024056	0.004024		
ρ_5	0.974961	0.547412	0.049352	
ρ_6	0.000983	0.448564	0.949897	0.538274
ρ_7			0.000751	0.359720
ρ_8				0.102006
σ^*	1.1220	1.1323	1.1440	1.1468
$\left(\frac{E_b}{N_0}\right)^* dB$	0.7611	0.6817	0.5924	0.5712

fading channel with SI. Similar to the rate-$1/2$ case, the thresholds of the degree distribution pairs approach the corresponding channel capacities. The threshold of the degree distribution pair optimized for the AWGN channel with $d_{l\max} = 50$ is only 0.07 dB away from the channel capacity. The threshold of the degree distribution pair with $d_{l\max} = 50$ optimized for the fading channel with SI is only 0.08 dB away from the capacity of the corresponding channel. Again, we compare both classes of rate-$1/3$ degree distribution pairs on the AWGN channel and the fading channel with SI in Figs. 6 and 7, respectively. It turns out that, as for rate-$1/2$ degree distribution pairs, the rate-$1/3$ degree distribution pairs optimized for the fading channel with SI are also very good distribution pairs for the AWGN channel and vice-versa.

B. BER Simulation Results

As shown in Fig. 3, the threshold values precisely predict the asymptotic performance as the block length of the LDPC codes approaches infinity. We are also interested in the performance of the optimized irregular LDPC codes when finite block size is considered. In the following results, we considered four rate-$1/3$ LDPC codes at a block size of 3072. The first one, LDPC ir1, is constructed according to the degree distribution pair with $d_{l\max} = 16$ optimized for the AWGN channel, as shown in Table II. The degree distribution pair has thresholds of -0.32 dB and 0.78 dB on the AWGN channel and the fading channel with SI, respectively. Note that the capacities for these two channels are -0.495 dB and 0.488 dB, respectively. The second one, LDPC ir2, is constructed according to the degree distribution pair with $d_{l\max} = 16$ optimized for the fading channel with SI, as shown in Table III, with thresholds of -0.25 dB and 0.68 dB on the AWGN and fading channel with SI, respectively. The third one, LDPC ir3, is constructed according to a degree distribution pair[3] with $d_{l\max} = 16$, which has thresholds of -0.18 dB and 0.96 dB on the AWGN and fading channel with SI, respectively. The last one, a quasi-regular[4] LDPC code R with all bit nodes degree-3, half of the check nodes degree-4, and half of the check nodes degree-5, has thresholds of 0.85 dB and 2.13 dB on the AWGN channel and the fading channel with SI, respectively. Among the four codes, ir1, ir2, and ir3 are all very good codes on both the AWGN channel and the fading channel with SI, whereas ir1 has the best threshold on the AWGN channel and ir2 has the best threshold on the fading channel with SI. In the construction of the parity-check matrices for the three irregular LDPC codes, we made all the degree-2 nodes loop-free and all of them correspond to nonsystematic bits. For all four codes, we

[3]This degree distribution pair was taken from Sae-Young Chung's web site: http://truth.mit.edu/~sychung/gaopt.html, which is an irregular LDPC codes design applet for design of good LDPC codes on an AWGN channel. The design method assumes Gaussian message densities, which is suboptimal since it is not true for the messages passed from check nodes to bit nodes. However, it turns out that this approximation makes the design much faster, yet still very effective. Refer to [6] for details.

[4]For rate-$1/3$ (j, k) regular LDPC codes, if we choose $j = 3$, we cannot make k to be an integer by the constraints of (24). Therefore, we choose half of the check nodes degree-4 and half of the check nodes degree-5. We denote this code as a rate-$1/3$ *quasi-regular* LDPC code.

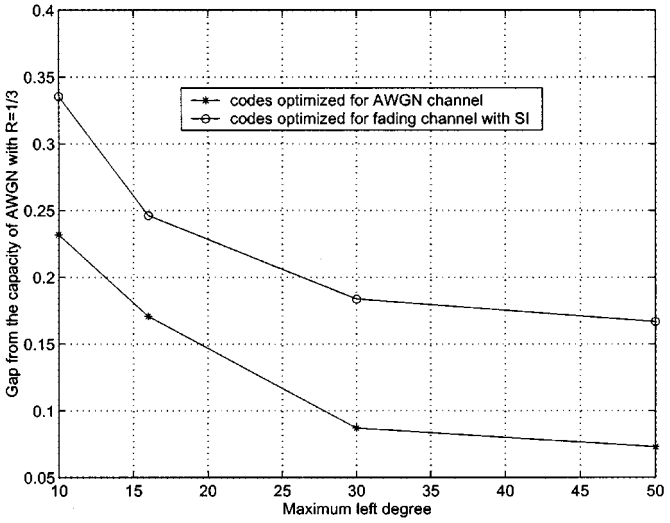

Fig. 6. Comparison of the threshold values on the AWGN channel of the rate-$1/3$ degree distribution pairs optimized for the AWGN channel and the fading channel with SI. For each distribution pair, the gap between its threshold value for the AWGN channel and the capacity of this channel is shown. Note that the capacity for the AWGN channel at rate $1/3$ is -0.4954 dB.

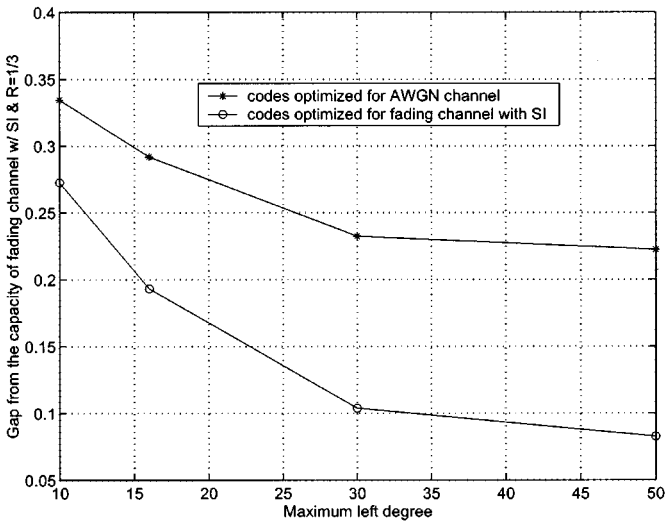

Fig. 7. Comparison of the threshold values on the fading channel with SI of the rate-$1/3$ degree distribution pairs optimized for the AWGN channel and the fading channel with SI. For each distribution pair, the gap between its threshold value for the fading channel with SI and the capacity of this channel is shown. Note that the capacity for the fading channel with SI at rate $1/3$ is 0.4885 dB.

avoided length-4 loops in the parity-check matrices. For the irregular codes, the bit error rates (BER) are given for systematic bits only. For the regular code, the BER is given for all bits.

Fig. 8 compares the simulation results of these four LDPC codes on both an AWGN channel and an uncorrelated Rayleigh fading channel with SI. It is shown that all three irregular LDPC codes achieve excellent performance on both channels. Note that the simulation results reflect the same relative performance as predicted by the computed threshold values. Furthermore, the irregular codes perform much better than the regular code. For example, at a BER of 2×10^{-4}, ir2 outperforms the regular LDPC code on the AWGN channel and fading channel with SI by about 0.7 dB and 1.0 dB, respectively.

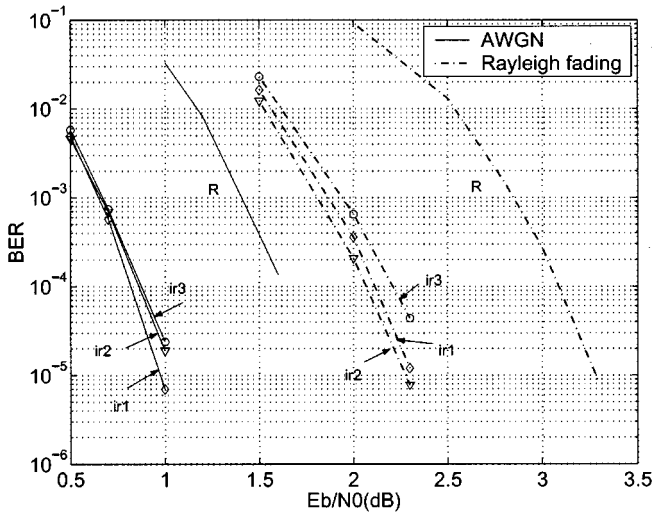

Fig. 8. Simulation of rate-$1/3$, block size 3072, quasi-regular LDPC code R, irregular LDPC codes ir1, ir2, and ir3 on both an AWGN channel and an uncorrelated Rayleigh fading channel with SI.

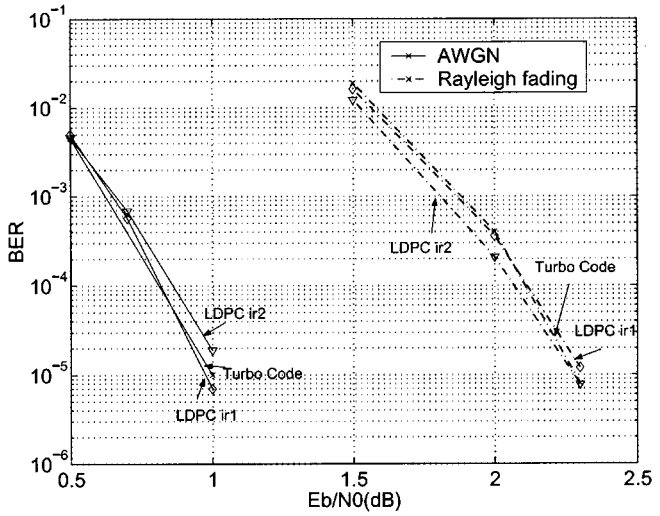

Fig. 9. Simulation of rate-$1/3$, block size 3072, Turbo code, irregular LDPC codes ir1 and ir2 on both an AWGN channel and an uncorrelated Rayleigh fading channel with SI.

In Fig. 9, ir1 and ir2 are compared to a $(1, 33/31, 33/31)$ turbo code [13] of the same block size and the same code rate on both an AWGN channel and an uncorrelated fading channel with SI. We can see that ir1 and ir2 achieve virtually the same performance as the turbo code. On the AWGN channel, ir1 is slightly better than the other two codes, while on the fading channel with SI, ir2 is slightly better.

Since both LDPC codes and turbo codes have excellent performance, they are being considered as potential candidates for mobile communications systems. The following results consider one such scenario—a land mobile channel with a delay constraint [13]. We assume the carrier frequency is 900 MHz, the source rate is 9.6 kb/s, the code rate is $1/3$, and the codeword block size is 3072. Therefore, the delay of the system is 106.7 ms. Three typical mobile speeds are considered: 4 m/h, 30 m/h, and 70 m/h; the corresponding normalized Doppler shifts $f_d T_s$ are $1.85 \times 10^{-4}, 1.39 \times 10^{-3}$, and 3.24×10^{-3},

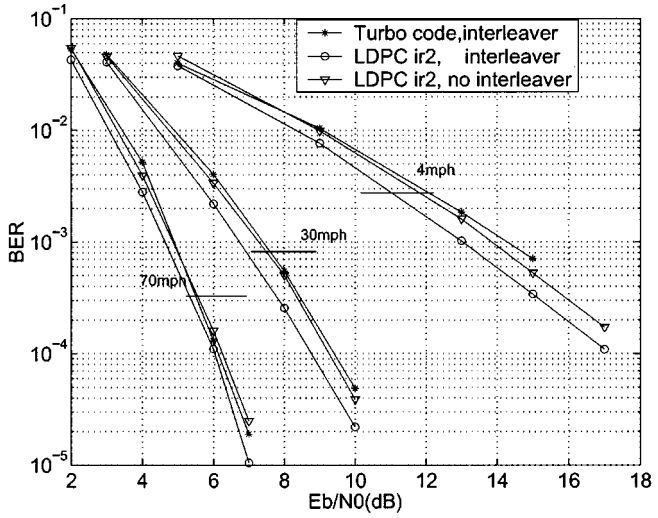

Fig. 10. Simulation of rate-$1/3$, block size 3072, turbo code with interleaver, irregular LDPC codes ir2 with and without interleaver on the correlated Rayleigh fading channel with SI, speed $= 4, 30$ and 70 mph.

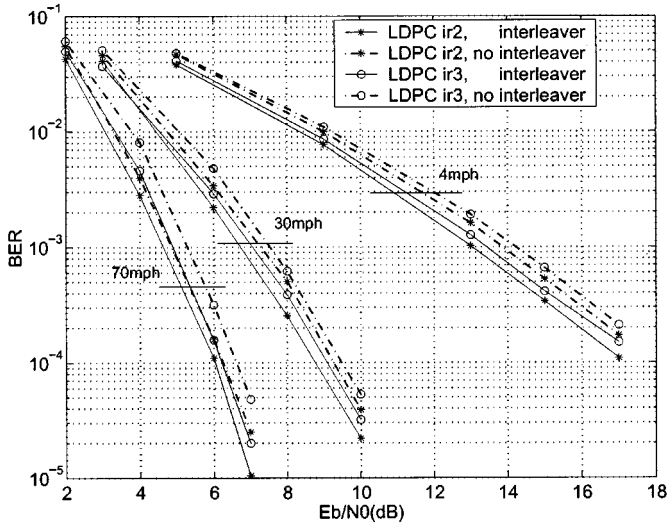

Fig. 11. Simulation of rate-$1/3$, block size 3072, irregular LDPC codes ir2 and ir3, both with and without interleaver on the correlated Rayleigh fading channels with SI, speed $= 4, 30$ and 70 mph.

respectively. Here, f_d is the Doppler shift, and T_s is the coded symbol duration. In our simulation work, a modified Jakes model [14] is used as the channel model. In the decoding of turbo codes, every bit needs to make use of the information of its neighbor bits to update its own likelihood information. Therefore, a channel block interleaver is introduced to break up the correlation of channel fades among the consecutive bits for the turbo coding schemes. However, in the decoding of LDPC codes, when bit n updates its related information from a parity check, e.g., check m, it only makes use of the information from those bits participating in check m. Because the parity-check matrix H of the LDPC code is randomly constructed, the probability that these bits will be the neighbors of bit n is very small. Therefore, when bit n is in a deep fade, it is very likely that some of these bits will not be in a deep fade and they can provide more reliable information for bit n. The random construction of the parity-check matrix and its sparseness property suggest that the decoder of LDPC codes has a built-in "interleaver," implying that LDPC codes should achieve very good performance on correlated fading channels even without using a channel interleaver.

In Fig. 10, three coding schemes are considered: a $(1, 33/31, 33/31)$ turbo code with a channel block interleaver, and LDPC code ir2 with and without a channel block interleaver. The same block interleaver is used for both codes, where the encoded symbols are read in row-by-row and read out column-by-column. At a speed of 70 m/h, the ir2 code with the interleaver performs the best. Interestingly, the ir2 code without the interleaver shows the same performance as the turbo code, and only suffers a loss of about 0.25 dB relative to the ir2 code with the interleaver. At a speed of 30 m/h, the ir2 code with the interleaver performs better than the turbo code by about 0.6 dB over a wide range of BER, and even the ir2 code without the interleaver shows slightly better results than the turbo code. When the speed of the mobile slows down to 4 m/h, the performance gap between the ir2 code with the interleaver and the turbo code becomes wider. At a BER of 10^{-3}, the ir2 code with the interleaver has as much as a 1.2 dB gain over the turbo code. The ir2 code without the interleaver still performs slightly better than the turbo code.

All these results demonstrate that, implicitly, there is a built-in "interleaver" in the parity-check matrix H. In principle, it is possible to design this "interleaver," i.e., to design the matrix H such that all the nonzero entries in H are distributed so as to achieve the maximal "interleaver" gain. Another conclusion drawn from these comparisons is that for fading channels with moderate-to-slow variations, that is, where less time diversity can be exploited from the coding schemes compared to the uncorrelated fading channel, the irregular LDPC codes can perform better than the turbo codes.

In Fig. 11, four coding schemes are compared: LDPC code ir2 with and without a channel block interleaver, and LDPC code ir3 with and without a channel block interleaver. As can be seen, the ir2 code with the interleaver always has a gain about $0.2 \sim 0.3$ dB over the ir3 code with the interleaver at any mobile speed considered here. Similar results can be observed for the ir2 code without the interleaver compared to the ir3 code without the interleaver. The results show that the LDPC codes which have better thresholds in the uncorrelated fading channel achieve better simulation performance in the correlated fading channels as well.

VII. Conclusion

In this paper, we have shown that the numerical analysis technique for calculating the threshold of the LDPC codes for the AWGN channel can be applied to the uncorrelated flat Rayleigh fading channel. In addition, using the nonlinear optimization technique of differential evolution, we optimized the degree distribution pairs for the uncorrelated Rayleigh fading channel and showed that their threshold values are extremely close to the capacity of this channel. Simulation results for moderate block size showed that the optimized LDPC codes can achieve excellent performance on the Rayleigh fading channel, and can outperform turbo codes on the correlated Rayleigh fading channels.

We also demonstrated that even without a channel interleaver, the LDPC codes still can achieve very good performance on correlated fading channels. This phenomenon may be a reflection of the built-in "interleaver" in the parity-check matrix H.

ACKNOWLEDGMENT

The authors wish to thank T. J. Richardson, R. Urbanke, S. Y. Chung, and H. D. Pfister for their helpful comments about the decoding analysis, and K. Tang for providing the simulation results for turbo codes.

REFERENCES

[1] T. J. Richardson and R. Urbanke, "The capacity of low-density parity-check codes under message-passing decoding," *IEEE Trans. Inform. Theory*, vol. 47, pp. 599–618, Feb. 2001.
[2] T. J. Richardson, A. Shokrollahi, and R. Urbanke, "Design of capacity-approaching irregular low-density parity-check codes," *IEEE Trans. Inform. Theory*, vol. 47, pp. 619–637, Feb. 2001.
[3] R. G. Gallager, *Low-Density Parity-Check Codes*. Cambridge, MA: MIT Press, 1963.
[4] M. G. Luby, M. Mitzenmacher, M. A. Shokrollahi, and D. A. Speilman, "Analysis of low density codes and improved designs using irregular graphs," in *Proc. ACM Symp.*, 1998, pp. 249–258.
[5] J. Pearl, *Probabilistic Reasoning in Intelligent Systems: Networks of Plausible Inference*. San Mateo, CA: Morgan Kaufmann, 1988.
[6] S. Y. Chung, R. Urbanke, and T. J. Richardson, "Analysis of sum-product decoding of low-density parity-check codes using a Gaussian approximation," *IEEE Trans. Inform. Theory*, vol. 47, pp. 657–670, Feb. 2001.
[7] R. Storn and K. Price, "Differential evolution—A simple and efficient heuristic adaptive scheme for global optimization over continuous spaces," *J. Global Optimization*, vol. 11, pp. 341–359, 1997.
[8] A. Shokrollahi and R. Storn, "Design of efficient erasure codes with differential evolution," in *Proc. IEEE Int. Symp. Information Theory*, Sorrento, Italy, June 2000, p. 5.
[9] D. J. C. MacKay, "Good error-correcting codes based on very sparse matrices," *IEEE Trans. Inform. Theory*, vol. 45, pp. 399–431, Mar. 1999.
[10] C. Berrou, A. Glavieux, and P. Thitimajshima, "Near Shannon limit error-correcting coding and decoding: Turbo codes," *Proc. IEEE Int. Conf. Commun.*, pp. 1064–1070, May 1993.
[11] J. Hagenauer, "Viterbi decoding of convolutional codes for fading- and burst-channels," in *Proc. Int. Zurich Seminar Digital Commun.*, Zurich, Switzerland, Mar. 1980, pp. 1–7.
[12] E. K. Hall and S. G. Wilson, "Design and analysis of turbo codes on Rayleigh fading channels," *IEEE J. Select. Areas Commun.*, vol. 16, pp. 160–174, Feb. 1998.
[13] K. Tang, P. H. Siegel, and L. B. Milstein, "On the performance of turbo coding for the land mobile channel with delay constraints," in *Proc. 33rd Asilomar Conf. SSC*, Pacific Grove, CA, Oct. 1999, pp. 1659–1665.
[14] P. Dent, G. E. Bottomley, and T. Croft, "Jakes fading model revisited," *IEE Electron. Lett.*, vol. 29, no. 13, pp. 1162–1163, June 1993.

Jilei Hou (S'00) received the B.E. degree (with highest honors) and M.E. degree in radio engineering from Southeast University, Nanjing, China, in 1995 and 1998, respectively. Since 1998, he has been pursuing the Ph.D. degree at the University of California, San Diego.

His research interests are in the areas of communication theory, information theory, channel coding, and spread-spectrum.

Paul H. Siegel (M'82–SM'90–F'97) received the B.S. degree in mathematics in 1975 and the Ph.D. degree in mathematics in 1979, both from the Massachusetts Institute of Technology, Cambridge, MA. He held a Chaim Weizmann fellowship during a year of postdoctoral study at the Courant Institute, New York University, New York.

He was with the IBM Research Division from 1980 to 1995. He joined the Faculty of the School of Engineering, University of California, San Diego in July 1995, where he is currently Professor of Electrical and Computer Engineering. He is affiliated with the Center for Wireless Communications and became Director of the Center for Magnetic Recording Research in September 2000. His primary research interest is the mathematical foundations of signal processing and coding, especially as applicable to digital data storage and communications. He holds several patents in the area of coding and detection for digital recording systems.

Prof. Siegel was a co-recipient of the 1992 IEEE Information Theory Society Paper Award and the 1993 IEEE Communications Society Leonard G. Abraham Prize Paper Award. He was a member of the Board of Governors of the IEEE Information Theory Society from 1991 to 1996. He served as Co-Guest Editor of the May 1991 Special Issue on "Coding for Storage Devices" of the IEEE TRANSACTIONS ON INFORMATION THEORY, and was an Associate Editor for Coding Techniques from 1992 to 1995. Prof. Siegel is a member of Phi Beta Kappa.

Laurence B. Milstein (S'66–M'68–SM'77–F'85) received the B.E.E. degree from the City College of New York, NY, in 1964 and the M.S. and Ph.D. degrees in electrical engineering from the Polytechnic Institute, Brooklyn, NY, in 1966 and 1968, respectively.

From 1968 to 1974, he was with by the Space and Communications Group, Hughes Aircraft Company, and from 1974 to 1976, he was a Member of the Department of Electrical and Systems Engineering, Rensselaer Polytechnic Institute, Troy, NY. Since 1976, he has been with the Department of Electrical and Computer Engineering, University of California at San Diego, La Jolla, where he is a Professor and former Department Chairman, working in the area of digital communication theory with special emphasis on spread-spectrum communication systems. He has also been a consultant to both government and industry in the areas of radar and communications.

Dr. Milstein was an Associate Editor for Communication Theory for the IEEE TRANSACTIONS ON COMMUNICATIONS, an Associate Editor for Book Reviews for the IEEE TRANSACTIONS ON INFORMATION THEORY, an Associate Technical Editor for the IEEE COMMUNICATIONS MAGAZINE, and the Editor-in-Chief of the IEEE JOURNAL ON SELECTED AREAS IN COMMUNICATIONS. He was the Vice President for Technical Affairs in 1990 and 1991 of the IEEE Communications Society and has been a member of the Board of Governors of both the IEEE Communications Society and the IEEE Information Theory Society. He has been a Member of the IEEE Fellows Selection Committee since 1996, and he currently is the Chair of that committee. He is also the Chair of ComSoc's Strategic Planning Committee. He is a recipient of the 1998 MILCOM Long-Term Technical Achievement Award, an Academic Senate 1999 UCSD Distinguished Teaching Award, an IEEE Third Millennium Medal, and the 2000 IEEE Communications Society Edwin Armstrong Achievement Award.